Spurious Modes of the TLM-Condensed Node Formulation

John Nielsen

Abstract—**The TLM method is based on temporal and spatial sampling of electromagnetic fields. As with the FD-TD method, this results in dispersive effects and propagating spurious modes that corrupt the field solution. The general dispersion relation for the TLM condensed node is used to quantify the propagation attributes of these spurious modes.**

I. Introduction

THE TLM method, is a means of simulating the solution to Maxwell's equations in an arbitrary bounded problem by modeling electrical properties of the bounded medium by an equivalent LCRG electrical circuit [1]–[5]. The 3-D TLM condensed node formulation was developed by P. Johns [6]. As with any numerical method that relies on spatial and time sampling, the condensed node has undesired dispersion associated with it. The dispersion characteristics of the condensed node are generally superior in comparison to the leap-frog FD-TD scheme developed by Yee [7] and the expanded TLM node [4] given similar node densities. A derivation of the dispersion equation for the condensed node, demonstrating this, is given in [8].

In addition to dispersion, spurious modes are generated in spatially sampled schemes. Signal corruption resulting from spurious modes in the FD-TD method was discussed by Trefethen [9]. In this letter the propagating and evanescent spurious modes of the condensed TLM node formulation are derived and discussed. When the condensed node mesh is applied to problems involving scattering or source structures that have feature dimensions of several lattice spacings, high-order spatial modes are generated. These modes suffer significant dispersion effects as outlined in [8]. If the spatial frequency of the mode is sufficiently high, it will propagate as a spurious mode with an incorrect propagation constant and in some cases with no loss. Spurious modes may have positive or negative group velocities.

II. Dispersion Relation of the Condensed TLM Node

The TLM condensed node lattice is a cubic structure with nodes placed at regular intervals of dimension "d." The interconnecting lines, joining adjacent nodes, are dispersionless transmission lines with a propagation constant denoted by k_o. The update time interval of the mesh is set equal to the time delay of a signal propagating from one node to the next, through an interconnecting transmission line.

The general dispersion relation for the condensed node mesh is based on application of Floquet's theorem to an infinite three-dimensional mesh. A plane wave solution is assumed with component propagation constants of k_x, k_y, and k_z in the x, y, and z direction respectively. In its final form, the dispersion relation for the condensed node is given as [8]

$$\det\left(\boldsymbol{I} - \boldsymbol{TPS}\right) = 0, \tag{1}$$

which is an implicit function of k_o, k_x, k_y and k_z. $\boldsymbol{I}$ is a 12 by 12 identity matrix, $\boldsymbol{T}$ is given by

$$\boldsymbol{T} = e^{-jk_o d}\boldsymbol{I}.$$

$\boldsymbol{S}$ is the scattering matrix of the TLM condensed node given in [6]. Finally $\boldsymbol{P}$ is a matrix containing the propagation constants whose elements are zero except

$$P_{1,12} = P_{5,7} = e^{jk_y d}$$

$$P_{2,9} = P_{4,8} = e^{jk_z d}$$

$$P_{3,11} = P_{6,10} = e^{jk_x d}$$

$$P_{7,5} = P_{12,1} = e^{-jk_y d}$$

$$P_{8,4} = P_{9,2} = e^{-jk_z d}$$

$$P_{10,6} = P_{11,3} = e^{-jk_x d}.$$

III. Spurious Solutions to the Dispersion Equation

The dispersion relation is used to determine the propagation characteristics of an arbitrary plane wave in an infinite 3-D mesh. Consider first the solution of $k_x d$, $k_y d$, and $k_z d$ for a small value of $k_o d$. The solution is a sphere with a radius of approximately $2 \cdot k_o d$. The factor of 2 is due to the low frequency propagation velocity in the periodic TLM mesh, which is half the velocity of the interconnecting transmission lines [4]. There is no dispersion along the k_x, k_y, and k_z axes. However, along the diagonal, $k_x d = k_y d = k_z d$, the radius is slightly inflated, revealing some dispersion [8]. As $k_o d$ increases, the bulges of the solution surface around the diagonals grow proportionally larger.

Due to the spatial sampling imposed by the mesh along x, y and z, the solution to the dispersion relation is periodic along the $k_x d$, $k_y d$, and $k_z d$ axis. That is, if $k_x d$, $k_y d$, $k_z d$ is a solution to the dispersion relation for a particular

Manuscript received March 15, 1991.

The author is with MEL-Defense Systems Ltd., 1 Iber Road, Stittsville, ON, Canada K2S-1E6.

IEEE Log Number 9101739.

1051-8207/91/0800-0201$01.00

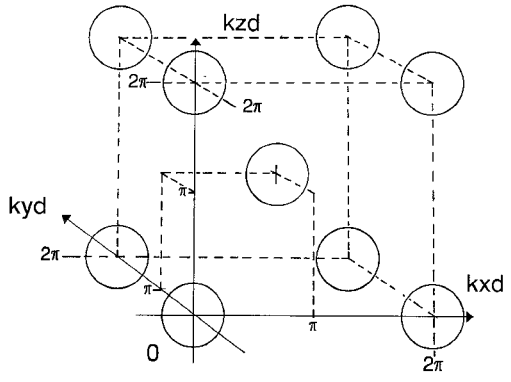

Fig. 1. Illustration of solution sphere satisfying the dispserion relation showing a body-centred-cubic structure.

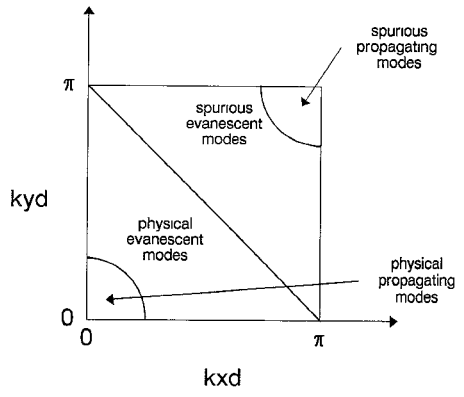

Fig. 2. Mode regions for TLM mesh model of a rectangular waveguide.

$k_o d$ then

$$k_x d + ii \cdot 2\pi, \qquad ii = \pm 1, \pm 2, \cdots,$$
$$k_y d + jj \cdot 2\pi, \qquad jj = \pm 1, \pm 2, \cdots,$$
$$k_z d + kk \cdot 2\pi, \qquad kk = \pm 1, \pm 2, \cdots,$$

are also solutions. Consequently, the solution sphere centered around $k_x d = k_y d = k_z d = 0$ is replicated in a cubic node pattern with a spacing of 2π. All these solution spheres do not contribute to spurious modes but are merely a consequence of spatial sampling.

In addition to the above solutions there is also a solution sphere centered at $k_x d = k_y d = k_z d = \pi$. This represents the spurious propagating mode solutions. As before, spurious solution spheres exist at intervals of 2π in $k_x d$, $k_y d$, and $k_z d$, due to spatial sampling. The total solutions, assuming $k_o d$ is small appears as a body-centred-cubic node structure as is shown in Fig. 1.

Attributes of spurious modes are best exemplified by considering mode propagation in a rectangular waveguide modeled by a TLM mesh. Assume an infinite homogeneous rectangular waveguide in the z direction that is modeled by a cubic condensed node mesh. The cross-section of the waveguide mesh model contains Nx nodes in the x direction and Ny nodes in the y direction. The ith column of nodes is located at $x = (i + 1/2)d$ and the jth row is located at $y = (j + 1/2)d$. The waveguide walls are assumed to be perfect conductors. The transverse propagation constants can then be expressed as

$$k_x d = \frac{n}{Nx}\pi, \qquad n = 0, 1 \cdots Nx,$$
$$k_y d = \frac{m}{Ny}\pi, \qquad n = 0, 1 \cdots Ny, \tag{2}$$

with the exception of modes $n = m = 0$ and $n = Nx$, $m = Ny$, which result in trivial solutions. Using the dispersion relation given in (1), $k_z d$ can be evaluated for each mode. The propagation characteristics of each mode falls into one of four regions as outlined in Fig. 2. The first region for small $k_x d$ and $k_y d$ is the "physical propagating modes." The propagating constant, $k_z d$, for these modes is real and close to the theoretical value of

$$k_z d = \sqrt{(2 \cdot k_o d)^2 - (k_x d)^2 - (k_y d)^2}. \tag{3}$$

Assuming an excitation frequency such that $k_o d$ is small relative to π, the boundary of this region is approximately circular, of a radius of 2 $k_o d$. As $k_o d$ increases, the boundary will bulge slightly around the diagonal $k_x d = k_y d$.

The adjacent region is denoted as the "physical evanescent modes," which have a purely imaginary $k_z d$ that increases in magnitude with the modal index as expected in actual waveguide modes. Near the physical mode cutoff boundary, the imaginary part of $k_z d$ follows (3) accurately provided $k_o d$ is reasonably small.

The propagation constant for modes that lie along the diagonal line given by

$$k_x d + k_y d = \pi$$

have an negative infinite imaginary component that indicates no propagation at all. Crossing this line such that

$$k_x d + k_y d > \pi,$$

the real part of $k_z d$ jumps to π. The modes in this region are denoted as the "spurious evanescent modes." In this region, the magnitude of the imaginary component of $k_z d$ decreases as the mode index increases.

The boundary between the spurious evanescent and propagating modes is a mirror image of the boundary separating the physical propagating and evanescent modes and is located approximately on the curve given by

$$2k_o d = \sqrt{(\pi - k_x d)^2 + (\pi - k_y d)^2}. \tag{4}$$

The spurious propagating modes have a propagation constant of approximately

$$k_z d \approx \pi \pm \sqrt{2k_o d - (\pi - k_x d)^2 - (\pi - k_y d)^2}, \tag{5}$$

which is purely real indicating lossless propagation. Note the constant offset factor of π. The upper sign in (5) denotes the forward propagating spurious mode and the lower sign the backward propagating mode.

Fig. 3 shows the real and imaginary parts of $k_z d$ as a function of $k_x d$ for $k_x d = 0$ to $k_x d = \pi$, with $k_y d = k_x d$. In this example, $k_o d$ is chosen to be 0.3. For small values of $k_x d$, $k_z d$ is real until the cutoff point at $k_x d = 0.42$. In Fig. 3(a), the theoretical solution of (3) is superimposed and is indistinguishable from the curve given by the dispersion

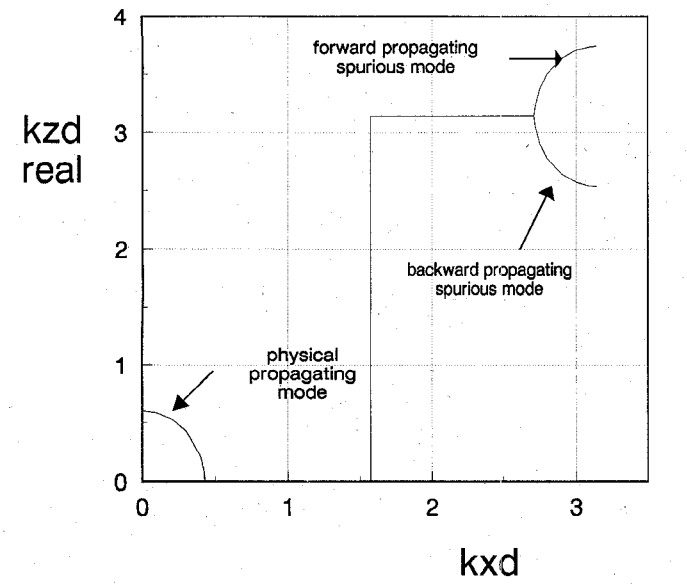

(a)

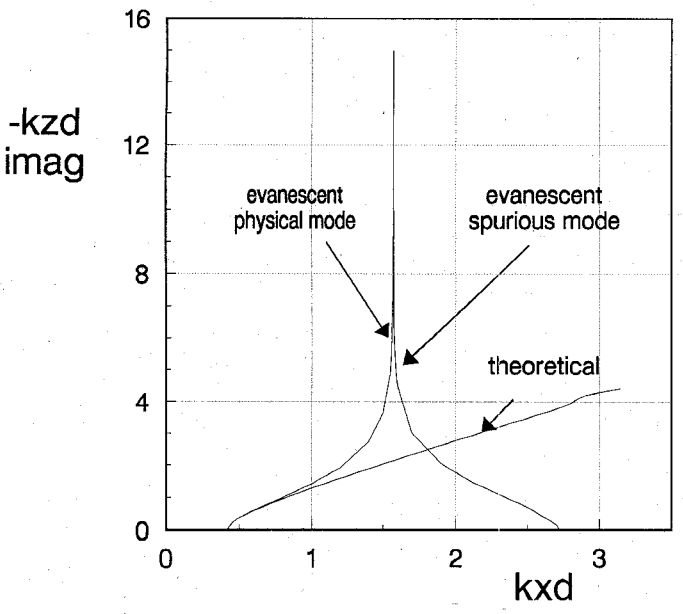

(b)

Fig. 3. Plot of $k_z d$ as a function of $k_x d$ with $k_o d = 0.3$ and $k_y d = k_x d$. (a) Real part. (b) Imaginary part.

relation, (1). At $k_x d = \pi/2$, the real part of $k_z d$ jumps to a value of π. At the cutoff point of the spurious mode, given by

$$k_x d = \pi - 0.42,$$

the spurious mode begins to propagate. The curves are shown in Fig. 3(a) for the cases of forward and backward propagation.

The imaginary part of $k_z d$ is shown in Fig. 3(b). When $k_x d$ exceeds the cutoff point, the mode becomes evanescent. It follows the theoretical curve, given by (3), reasonably closely until $k_x d$ approaches $\pi/2$. Beyond the discontinuity, the mode become spurious. At the spurious mode cutoff, the imaginary part of $k_z d$ becomes zero.

Acknowledgment

Acknowledgments are due to S. Charland of Lockheed Canada Inc. and G. Costache of the University of Ottawa for reviewing the letter.

References

[1] P. B. Johns and R. L. Beule, "Numerical solution of two-dimensional scattering problems using a transmission-line matrix," *Proc. Inst. Electr. Eng.*, vol. 118, Sept. 1971, pp. 1203–1208.

[2] S. Akhtarzad, "Analysis of lossy microwave structures and microstrip resonators by the TLM method," Ph.D. dissert., Univ. of Nottingham, England, July 1975.

[3] P. Saguet, "Analyse des milieux guidès: la méthode MTLM," Doctoral thesis, Inst. Natl. Polytech., Genoble, France, 1985.

[4] W. J. R. Hoefer, "The transmission line method—Theory and application," *IEEE Trans. Microwave Theory Tech.*, vol. MTT-33, no. 10, pp. 882–893, Oct. 1985.

[5] ——, "The transmission line matrix (TLM) method," *Numerical Techniques for Microwave and Millimeter-Wave Passive Structure*, T. Itoh, Ed. New York: John Wiley, 1989, ch. 8.

[6] P. B. Johns, "A symmetrical condensed node for the TLM method," *IEEE Trans. Microwave Theory Tech.*, vol. MTT-35, no. 4, pp. 370-377, Apr. 1987.

[7] K. S. Yee, "Numerical solution of initial boundary value problems involing Maxwell's equations in isotropic media," *IEEE Trans. Antennas Propag.*, vol. AP-14, pp. 302–307, May 1966.

[8] J. Nielsen and W. J. R. Hoefer, "A complete dispersion analysis of the condensed node TLM mesh," presented at *IEEE CEFC'90 Conf.*, Oct. 1990.

[9] L. N. Trefethen, "Group velocity in finite difference schemes," *SIAM Rev.*, vol. 24, no. 2, pp. 113–135, Apr. 1982.